



Published in final edited form as:

Shock. 2016 October ; 46(4): 420–430. doi:10.1097/SHK.0000000000000605.

## **<sup>99m</sup>Tc-Hexamethylpropyleneamine Oxime Imaging for Early Detection of Acute Lung Injury in Rats Exposed to Hyperoxia or Lipopolysaccharide Treatment**

**Said H. Audi<sup>1,2,7</sup>, Anne V. Clough<sup>2,3,7</sup>, Steven T. Haworth<sup>2</sup>, Meetha Medhora<sup>2,4</sup>, Mahsa Ranji<sup>5</sup>, John C. Densmore<sup>6</sup>, and Elizabeth R. Jacobs<sup>2,7</sup>**

<sup>1</sup>Department of Biomedical Engineering, Marquette University

<sup>2</sup>Division of Pulmonary and Critical Care Medicine, Medical College of Wisconsin

<sup>3</sup>Department of Mathematics, Statistics, and Computer Science, Marquette University

<sup>4</sup>Department of Radiation Oncology, Medical College of Wisconsin

<sup>5</sup>Department of Electrical Engineering, University of Wisconsin-Milwaukee

<sup>6</sup>Department of Surgery, Medical College of Wisconsin

<sup>7</sup>Zablocki V.A. Medical Center

### **Abstract**

<sup>99m</sup>Tc-Hexamethylpropyleneamine oxime (HMPAO) is a clinical single-photon emission computed tomography biomarker of tissue oxidoreductive state. Our objective was to investigate whether HMPAO lung uptake can serve as a pre-clinical marker of lung injury in two well-established rat models of human acute lung injury (ALI).

Rats were exposed to >95% O<sub>2</sub> (hyperoxia) or treated with intratracheal lipopolysaccharide (LPS), with first endpoints obtained 24 hours later. HMPAO was administered intravenously before and after treatment with the glutathione-depleting agent diethyl maleate (DEM), scintigraphy images were acquired, and HMPAO lung uptake was quantified from the images. We also measured breathing rates, heart rates, oxygen saturation, bronchoalveolar lavage (BAL) cell counts and protein, lung homogenate glutathione (GSH) content, and pulmonary vascular endothelial filtration coefficient ( $K_f$ ).

For hyperoxia rats, HMPAO lung uptake increased after 24 hours (134%) and 48 hours (172%) of exposure. For LPS-treated rats, HMPAO lung uptake increased (188%) 24 hours after injury and fell with resolution of injury. DEM reduced HMPAO uptake in hyperoxia and LPS rats by a greater fraction than in normoxia rats. Both hyperoxia exposure (18%) and LPS treatment (26%) increased lung homogenate GSH content, which correlated strongly with HMPAO uptake. Neither of the treatments had an effect on  $K_f$  at 24 hours. LPS-treated rats appeared healthy but exhibited mild tachypnea, BAL and histological evidence of inflammation, and increased wet and dry lung

---

**Corresponding Author: Said H. Audi, Ph.D.**, Research Service 151, Zablocki VAMC, 5000 W. National Ave., Milwaukee, WI 53295, Phone: 414-384-2000 ext. 41452, FAX: 414-384-0115, said.audi@mu.edu.

### **FINANCIAL DISCLOSURE**

Nothing to disclose.

weights. These results suggest the potential utility of HMPAO as a tool for detecting ALI at a phase likely to exhibit minimal clinical evidence of injury.

### Keywords

Acute lung injury; lung imaging; hyperoxia; endotoxin; SPECT

## INTRODUCTION

Acute lung injury (ALI) is characterized by rapidly progressing hypoxic lung failure following a direct or indirect injury to the pulmonary parenchyma or vasculature (1). This condition is one of the most frequent complications encountered in patients admitted to medical intensive care units, and of the approximately one million patients receiving invasive mechanical ventilation per year, 25% who did not have ALI develop ALI (2). The most serious form of ALI is Acute Respiratory Distress Syndrome (ARDS) which occurs in ~200,000 patients in the U.S. per year and carries a mortality rate of nearly 40% despite the best supportive care (1).

Rat exposure to lethal hyperoxia (>95% O<sub>2</sub>) or intratracheal endotoxin (lipopolysaccharide, LPS) comprise two well-established animal models of human ALI/ARDS (3–5). Both hyperoxia and LPS reproduce the cardinal features of clinical ALI/ARDS, namely bilateral infiltrations on chest roentgenographic studies, decreased lung compliance, parenchymal injury including increased vascular permeability, low-pressure edema, and hypoxemia (3,4).

Crapo et al. (4) provide a detailed description of histologic and morphometric changes in lungs of rats exposed to lethal (>95% O<sub>2</sub>) hyperoxia. No structural or functional changes are observed in lungs of rats exposed to lethal hyperoxia for up to 40 hours. However, by 60 hours, there is a 30% loss in capillary endothelial cells and cell surface, infiltration of phagocytic leukocytes, and an increase in the thickness of air-blood barrier. Further loss in endothelial cells and edema, and an increase in the thickness of the air-blood barrier, pleural effusion, severe hypoxemia and death follow within 72 hours.

Previous studies have demonstrated that rat intratracheal (IT) treatment with LPS induces dose-dependent lung functional, histological, and cellular changes consistent with those observed with clinical sepsis (5,6). For low LPS doses (< 5 mg/kg), lung injury peaks around 24 hrs and is reversible (5,6).

Oxidative stress and inflammation are common pathways in the pathogenesis of hyperoxia and LPS-induced ALI (3,7). In particular, endothelial apoptosis (7–9), mitochondrial dysfunction (7–12), and altered lung tissue oxidoreductive state (13,14) are features of both disorders. Furthermore, there is strong evidence that the pulmonary capillary endothelium is a primary and initial site of both hyperoxia- and LPS-induced ALI (4,7,11). This vulnerability and the large pulmonary capillary endothelium surface area in direct apposition with blood-borne compounds suggest the utility of biomarker imaging for detecting lung endothelial injury following hyperoxia or LPS exposure (8,9,14).

The single-photon emission computed tomography (SPECT) biomarker technetium-labeled hexamethylpropyleneamine oxime ( $^{99m}\text{Tc}$ -HMPAO) was originally developed as a brain perfusion agent but its uptake and retention in several tissues serves as a marker of tissue redox state (15). Uptake from the circulation is dependent on its rate of diffusion across the plasma membrane (15). Once intracellular, HMPAO can either diffuse back to the interstitial/vascular region, or be reduced to its hydrophilic, non-diffusible form and retained within cells (15). HMPAO reduction and thus its cellular retention, has been shown to be strongly dependent on the oxidoreductive state of the tissue including intracellular glutathione (GSH) content and other factors involving mitochondrial function (15).

Previously we demonstrated that the lung uptake of HMPAO is differentially altered in rats preconditioned to induce increased or decreased susceptibility to the otherwise lethal effects of prolonged exposure to lethal hyperoxia (14). We also used  $^{99m}\text{Tc}$ -HMPAO along with  $^{99m}\text{Tc}$ -duramycin (DU) a SPECT biomarker of tissue injury sensing cell death via apoptosis and/or necrosis, to identify the different stages of lung  $\text{O}_2$  toxicity in rats exposed to sublethal hyperoxia (85%  $\text{O}_2$ ) for 21 days (9). The lung uptake of both DU and HMPAO increased during the inflammatory phase (days 3–7). Thereafter HMPAO lung uptake leveled off and remained elevated during the adaptation phase (> 7 days), whereas DU uptake decreased to near control levels by 21 days (9).

Roughly 70% of ALI patients are not recognized as such on presentation by bedside providers (16). Experts stress the importance of early detection of ALI (i.e. prior to evidence of clinical respiratory distress) for enhancing the efficacy of existing therapies and improving outcomes of ALI/ARDS patients (16). Thus, our long-term goal is to develop a means for early clinical detection and monitoring of ALI in individual patients. To that end, the main objective of the present study was to determine whether  $^{99m}\text{Tc}$ -HMPAO lung uptake can serve as a marker of lung injury at a time point likely to exhibit minimal clinical evidence of injury in two rat models of human ALI/ARDS, namely rat exposure to lethal hyperoxia (>95%  $\text{O}_2$ ) or intratracheal (IT) treatment with a low LPS dose (1 mg/kg). Another objective was to evaluate the ability of HMPAO lung uptake to track lung injury progression with sustained exposure to lethal hyperoxia, and reversibility following treatment with LPS.

## MATERIALS AND METHODS

### Materials

HMPAO (Ceretek®) was purchased from GE Healthcare (Arlington Heights, IL), and technetium-labeled macroaggregated albumin ( $^{99m}\text{Tc}$ -MAA, particle sizes 20 – 40  $\mu\text{m}$ ) was purchased from Cardinal Health (Wauwatosa, WI). Antibody to myeloperoxidase (MPO) (Abcam # Ab9535) was used with secondary antibody (Abcam #6829 HRP) to identify MPO positive cells. Diethyl maleate (DEM) and other reagent grade chemicals were purchased from Sigma-Aldrich (St. Louis, MO).

## Rat models of ALI

All treatment protocols were approved by the Institutional Animal Care and Use Committees of the Zablocki Veterans Affairs Medical Center, the Medical College of Wisconsin and Marquette University (Milwaukee, WI).

For normoxia (control) rat studies, adult (68–77 days old) male Sprague-Dawley rats (Charles River;  $323 \pm 4$  (SEM) g,  $n = 24$ ) were exposed to room air in chambers side by side with those exposed to hyperoxia. For hyperoxia studies, rats within the same weight ( $341 \pm 3$  g,  $n = 55$ ) and age range of normoxia rats were housed in a Plexiglass chamber maintained at  $>95\%$   $O_2$  for 24 hrs ( $n = 32$ ) or 48 hours ( $n = 23$ ) as described (14).

For LPS and saline (LPS vehicle) studies, rats ( $336 \pm 5$  g,  $n = 56$  for LPS;  $331 \pm 9$ ,  $n = 29$  for saline) were anesthetized with isoflurane (0.5%–3%). The vocal cord was then visualized and LPS (1 mg/kg in 0.25 ml sterile saline) or sterile saline (0.25 ml) was introduced into the lungs using a micro-sprayer (Penn-Century, Philadelphia, PA, USA) (17). The rats recovered from anesthesia and were studied 24 hours ( $n = 41$ ), 3 days ( $n = 8$ ), or 7 days ( $n = 7$ ) later.

## Breathing rate

Breathing rates were measured in room air via plethysmography as previously published by us (18). Rats were placed in a transparent box connected to a differential pressure transducer. The mean breathing rate in each rat was calculated from a minimum of four steady regions of recording lasting at least 15 seconds each. Measurements were acquired in 10–15 minutes, after which time rats in hyperoxia were returned to the high oxygen environment.

## Heart rate and oxygen saturation measurements

Heart rate and oxygen saturation were measured in non-anesthetized rats using a veterinary pulse oximeter (Nonin, 8600V series, Plymouth, MN, USA) connected to a computer with WinDaq data acquisition and analysis software (18). A probe was positioned over the tail artery in gently restrained rats, and recordings from the oximeter were acquired over several minutes. Steady traces with 2–4 ten-second stable pulse readings in the physiological range were acquired from each rat and analyzed by an operator blinded to the treatment of the rat.

## Chest X-ray images

Representative rats from normoxia, 24-hr hyperoxia, 24-hr saline, and 24-hr LPS groups were anesthetized with pentobarbital (50 mg/kg). Chest X-rays were then acquired using a microfocal X-ray system (Feinfocus FXE 0.20) with 0.25 second exposure time, 70 kVp voltage, and 30  $\mu$ A current. Images were compared by a trained investigator masked to the treatment group (STH).

## Bronchoalveolar lavage (BAL)

Representative rats from normoxia, 24-hr hyperoxia, 24-hr saline, and 24-hr LPS groups were anesthetized intraperitoneally with Beuthanasia (40–50 mg/kg i.p.). The trachea was surgically exposed and cannulated. The excision was extended caudally to open the chest and the heart and lungs were removed from the thoracic cavity. The lungs were infused

through the trachea with a total volume of 3 ml of iced phosphate-buffered saline with no added calcium *ex vivo* (19). The solution was withdrawn and saved for analysis, and the procedure was repeated with a second volume of 3 ml for a total instilled lavage of 6 ml (19).

**Cell counts and cytopins**—The returned BAL volume was measured, then 1 ml was removed for determination of total cell counts and protein concentration in the cell-free supernatant. The remainder of the sample was used for cytopsin preparations. Cell counts were obtained by resuspending the cell pellet from 1 ml after centrifugation at 1000 g for 10 minutes in a known volume and counting with a hemocytometer. Cytopsin preparations were prepared from the BAL fluid using a standard clinical protocol (19).

Differential counts were obtained from high resolution JPEG images of Papanicolaou-stained cytopsin analyzed by a clinician (ERJ) who was blinded to the identity of each sample. The cytopsin image was divided into six sections. A region of interest roughly 0.5 mm x 0.5 mm within each section was selected at low power. Differential cell distributions were determined at 200X power on a minimum of 100 and maximum of 200 cells per BAL sample. Depending on cell density, between three and six of the regions detailed above were analyzed.

### Lung wet-to-dry weights

Heart and lungs from a randomly selected subset of each of the groups of rats were isolated and washed free of blood using the isolated perfused lung preparation described below for filtration coefficient measurements. After washing, the lungs were dissected free of the heart, trachea and mainstem bronchi and total lung wet weight was obtained. The left lung lobe was weighed and dried at 60°C for wet-to-dry weight ratio and the remaining lung lobes were used for glutathione assays or for the histological studies described below.

### Isolated perfused lung (IPL) preparation and pulmonary vascular endothelial filtration coefficient ( $K_f$ )

Representative rats from normoxia, 24-hr hyperoxia, 48-hr hyperoxia, 24-hr saline, and 24-hr LPS groups were anesthetized with Beuthanasia (40–50 mg/kg i.p.). The trachea was surgically isolated and cannulated, the chest opened and heparin (0.7 IU/g body wt.) injected into the right ventricle as previously described (14). The pulmonary artery and the pulmonary venous outflow were accessed via cannula. The lung was removed and suspended from a calibrated force displacement transducer (Model FT03; Grass Instruments) and lung weight was monitored continuously. The Krebs-Ringer bicarbonate perfusate contained (in mM) 4.7 KCl, 2.51 CaCl<sub>2</sub>, 1.19 MgSO<sub>4</sub>, 2.5 KH<sub>2</sub>PO<sub>4</sub>, 118 NaCl, 25 NaHCO<sub>3</sub>, 5.5 glucose, and 5% bovine serum albumin. The perfusion system was primed (Masterflex roller pump) with the perfusate maintained at 37°C and equilibrated with 15% O<sub>2</sub>, 6% CO<sub>2</sub>, balance N<sub>2</sub> gas mixture resulting in perfusate PO<sub>2</sub>, PCO<sub>2</sub> and pH of ~105 Torr, 40 Torr, and 7.4, respectively. The lung was ventilated (40 breaths/min) with the above gas mixture with end-inspiratory and end-expiratory pressures of ~ 6 and 3 mmHg, respectively. The pulmonary arterial and venous pressures were referenced to atmospheric pressure at the level of the left atrium and monitored continuously during the course of the experiments.

Perfusate was pumped (0.03 ml/min/g body weight) through the lung until it was evenly blanched and venous effluent was clear of visible blood before switching from single pass to recirculation mode.

The value of  $K_f$ , a measure of vascular permeability, was determined using the approach described by Bongard et al. (20). After a 10 min stabilization period with the venous pressure ( $P_V$ ) set at atmospheric pressure,  $P_V$  was raised to 3.7 mmHg and the lung perfused for 10 min. Then,  $P_V$  was raised to 10 mmHg and perfusion continued for an additional 10 min.  $K_f$  was determined by dividing the difference in the rate of lung weight gain measured 10 min after increasing  $P_V$  from 3.7 to 10 mmHg and after increasing  $P_V$  from 0 to 3.7 mmHg by the difference in pulmonary capillary pressure at these  $P_V$  values. For each  $P_V$ , the capillary pressure was estimated as the average of arterial and venous pressures.  $K_f$  was normalized to gram of dry lung weight.

### Histological studies

In a randomly selected subset of normoxia, 24-hr hyperoxia, 24-hr saline-treated, and 24-hr LPS-treated rats, lungs were fixed inflated in 10% neutral buffered formalin (Fisher Scientific, Pittsburg, PA) and embedded in paraffin. Whole-mount sections of lung were cut (4  $\mu$ m thick whole mounts), processed and stained with Hematoxylin & Eosin (H&E, Richard Allan, Kalamazoo, MI) or myeloperoxidase (MPO; Abcam Ab9535 1:100), the latter after deparaffinization and antigen retrieval.

Using high resolution jpeg images of the slides, an investigator masked to the treatment groups obtained six representative images from each slide (10X for H&E and 20X for MPO) avoiding large vessels or airways. These images were then scored independently by two investigators blinded to the treatment groups. For grading of H&E, we used a 0–3 scoring system for epithelial, inflammatory and fibrotic changes (21): 0 = no inflammation; 1 = mild perivascular or peribronchiolar inflammatory infiltrates; 2 = moderate mixed inflammatory infiltrates throughout the lung; 3 = severe infiltration of mixed inflammatory cells. For MPO studies undertaken to better define inflammatory cell infiltrates, the number of brown (positive) cells per field was counted.

### Imaging studies

Rat imaging studies described below were conducted for a randomly selected subset of each of the groups (see results for the number of rats for each group).

$^{99m}\text{Tc}$ -HMPAO was constituted and labeled according to kit directions, while  $^{99m}\text{Tc}$ -MAA was obtained in its labeled form. Rats were anesthetized with pentobarbital sodium (40–50 mg/kg, i.p.) and a femoral vein was cannulated. The rat was then placed supine on a plexiglass plate (4 mm) positioned directly on the face of a parallel-hole collimator (hole diameter = 2 mm, depth = 25 mm) attached to a modular gamma camera (*Radiation Sensors, LLC*) for planar imaging (9,14). An injection of  $^{99m}\text{Tc}$ -HMPAO (37–74 MBq) was administered via the femoral vein catheter. The injected dose was calculated from the difference between the pre- and post- injection activity within the syringe using a dose calibrator. At 15 minutes post-injection, a one-minute planar image was acquired (9,14).

To investigate the role of GSH in the lung retention of  $^{99m}\text{Tc}$ -HMPAO, rats were then treated with the GSH-depleting agent diethyl maleate (DEM) (1g/kg BW i.p.) and after 45 minutes a second injection of  $^{99m}\text{Tc}$ -HMPAO was made and the animal reimaged 15 minutes later (14). DEM depletes GSH by conjugating with it to form a thioether conjugate via a reaction catalyzed by the enzyme glutathione-S-transferase (14). Again, without relocation of the rat, a third injection, this time of  $^{99m}\text{Tc}$ -MAA (37 MBq), was made via the same cannula and the rat re-imaged. The  $^{99m}\text{Tc}$ -MAA injection provided a planar image in which the lung boundaries were clearly identified, since >95% of  $^{99m}\text{Tc}$ -MAA lodged in the lungs. After imaging, the rats were euthanized with an overdose of pentobarbital sodium. For a subset of these imaged rats, the lungs were removed, fixed inflated with paraformaldehyde, and then following  $^{99m}\text{Tc}$  decay, used for histological studies described above.

### Image analysis

Images were analyzed using MATLAB-based software developed in-house. The boundaries of the upper portion of the lungs were identified in the high-sensitivity  $^{99m}\text{Tc}$ -MAA images and manually outlined to construct a lung region of interest (ROI) free of liver contribution (9,14). The  $^{99m}\text{Tc}$ -MAA lung ROI mask was then superimposed on the  $^{99m}\text{Tc}$ -HMPAO images yielding a lung  $^{99m}\text{Tc}$ -HMPAO ROI. No registration was required since the animal was maintained in the same location throughout the imaging study. Background regions in the upper forelimbs were also identified in the  $^{99m}\text{Tc}$ -HMPAO images to normalize lung activity for injected  $^{99m}\text{Tc}$ -HMPAO specific activity, dose, and decay (9). Mean counts/sec/pixel/injected dose within both the lung and forelimb-background ROIs were then determined and decay corrected. The ratio of the lung and background ROI signals averaged over the 15 – 20 minute time interval, when the  $^{99m}\text{Tc}$ -HMPAO signal within the ROIs had reached steady state, was used as the measure of lung steady-state  $^{99m}\text{Tc}$ -HMPAO uptake (9,14). The  $^{99m}\text{Tc}$ -HMPAO images acquired after DEM treatment were analyzed in the same way except that the pre-injection baseline activity level within each ROI was subtracted from the corresponding post-injection activity level to account for residual  $^{99m}\text{Tc}$ -HMPAO from the first injection (9).

### Glutathione (GSH) content

Lungs were isolated and washed free of blood using the Krebs-Ringer bicarbonate perfusate described above. Total lung wet weight was obtained then a fraction of the lung was used for the glutathione assay.

Lung tissue was dissected free from large airways and connective tissue and weighed. The tissue was then placed into 10 volumes (per lung wet weight) of 4°C sulfosalicylic acid (5%), minced, and homogenized. The homogenate was centrifuged (10,000 × g) at 4°C for 20 minutes, and the supernatant was used to determine reduced (GSH) and oxidized (GSSG) lung glutathione content as previously described (14,20).

### STATISTICAL ANALYSIS

Statistical evaluation of data was carried out using SigmaPlot version 12.0 (Systat Software Inc., San Jose, CA). For the imaging studies, sample sizes were chosen to achieve a power >

85% using power analysis (ANOVA power; SigmaPlot version 12.0) based on previously published results with  $^{99m}\text{Tc}$ -HMPAO (9,14). When several samples from the same rat were obtained (e.g. images of six fields for quantitation of MPO positive cells from a single rat), averages of these values were taken as an “n” of 1 for statistical comparisons. Values from different groups were compared using one way ANOVA. In some studies as indicated in the text such as comparison of HMPAO before and after DEM, paired *t*-test or Wilcoxon Signed Rank was employed. For studies with repeated measurements at more than two time points, one way repeated-measure ANOVA was used. The level of statistical significance was set at  $p < 0.05$ . Values for the histological scores of two graders were averaged, then performance of the groups compared by Kruskal-Wallis one way ANOVA on ranks. Values are mean  $\pm$  SEM or confidence intervals as indicated in the text unless otherwise indicated.

## RESULTS

### Body weights, breathing rates, heart rates, oxygen saturation, and chest X-ray

All rats in each of the treatment groups moved spontaneously about the cage, exhibited good condition of the fur, sought food and water actively, and had good skin turgor at the time of euthanasia. Posture and skin/mucous membrane color were normal. For rats exposed to hyperoxia, their initial body weight increased by  $1.9 \pm 0.3$  % (paired *t*-test,  $p < 0.001$ ) after 24 hrs, but decreased by  $2.2 \pm 0.5$  % (Wilcoxon Signed Rank Test,  $p < 0.001$ ) after 48 hrs (Table 1). For rats treated with IT saline, their initial body weight was unchanged by 24 hrs (Table 1). On the other hand, rats treated with LPS lost  $6.2 \pm 0.4$  % (paired *t*-test,  $p < 0.001$ ) of their initial body weight by 24 hrs accompanied by a decrease in their water (41%) and food (49%) intake. However, by 48 hrs after LPS treatment, their body weights and oral intake had recovered to baseline (Figure 1) and continued to rise after that time (Table 1).

Rat exposure to  $> 95\%$   $\text{O}_2$  for 24 hrs resulted in  $\sim 10\%$  decrease in breathing rate ( $123 \pm 11$  bpm at 0 hrs vs.  $110 \pm 3$  breaths per min (bpm) at 24 hrs) (one way repeated measure ANOVA,  $p < 0.005$ ) (Figure 1). Breathing rates after 48 hrs of hyperoxia exposure ( $104 \pm 3$  bpm) were not different from those after 24 hrs of exposure ( $110 \pm 3$  bpm). Treatment with IT saline had no effect on breathing rates ( $133 \pm 5$  (n = 6) bpm just before treatment vs.  $130 \pm 5$  bpm 24 hrs following treatment). Breathing rates increased in rats 24 hrs following treatment with LPS from  $123 \pm 2$  (n = 6) to  $172 \pm 9$  bpm (one way repeated measure ANOVA,  $p < 0.001$ ). Figure 1 shows that three days following treatment with LPS, breathing rates ( $122 \pm 5$  bpm) were not different from baseline or saline values.

Blood oxygen saturations 24 hrs after hyperoxia, IT saline, or IT LPS were not different from those of normoxia rats, consistent with a pulmonary reserve and capacity to compensate in the three treatment groups (Table 2). Rat exposure to hyperoxia for 48 hrs resulted in a small ( $\sim 2\%$ ) clinically irrelevant, but statistically significant decrease in oxygen saturation. Heart rates 24 hrs after hyperoxia or IT saline were not different from those of normoxia rats (Table 2). Twenty-four hrs after LPS treatment, there was a small ( $\sim 13\%$ ), but statistically significant decrease in heart rate as compared to that of normoxia but not that of IT saline rats (Table 2).



Based on blinded interpretation, there were no differences in the chest X-rays of rats 24 hrs after treatment with hyperoxia, saline, or LPS as compared to those of normoxia rats (not shown).

### Lung wet/dry weight ratios and filtration coefficients

Rat exposure to hyperoxia for 24 hrs had no effect on left lobe wet weight/body weight ratio or wet-to-dry weight ratio as compared to those for lungs of normoxia rats (Table 3). In contrast, rat exposure to hyperoxia for 48 hrs increased left lobe wet weight/body weight ratio by 31% ( $p < 0.001$ ) compared to that of normoxia rats (Table 1). The wet-to-dry weight ratio in this group was not different from that of normoxia rats. For LPS-treated rats, left lobe wet weight/body weight ratio increased by 44% ( $p < 0.001$ ) 24 hrs later as compared to that of saline-treated rats. However 3 days after LPS treatment, left lobe wet weight/body weight ratio were back to near values of saline-treated rats (Table 3). LPS treatment had no effect on lung wet-to-dry weight ratio (Table 3). The lung vascular endothelial filtration coefficients ( $K_f$ ) 24 hours after hyperoxia, IT saline, or LPS were not different from that for normoxia lungs (Table 3). However, rat exposure to hyperoxia for 48 hrs increased  $K_f$  by more than ~200% as compared to that for normoxia lungs (Table 3).

### Histology and BAL

Figure 2 depicts representative H&E stained lung images of normoxia rats and of rats 24 hrs after hyperoxia exposure, IT saline, or IT LPS. Images from normoxia rats show the lacey architecture of normal lungs with very thin alveolar capillary membranes to facilitate gas exchange. Scores of inflammation were not different in lungs from normoxia and hyperoxia rats with respect to inflammatory changes (H&E, Figure 2 and Table 4) or number of MPO positive cells (Figure 3, Table 5). Lungs from rats treated with LPS exhibited mild inflammatory changes and an increase in the number of MPO positive cells as compared to those of normoxia rats (see Figures 2–3 and Tables 4–5).

Protein concentrations in BAL from cohorts of rats that received IT saline and 24 hrs hyperoxia were not different from those of normoxia (Table 7). Protein concentrations in BAL from rats 24 hrs after LPS treatment were higher than those of the other three groups.

Total cell counts in BAL were identical in normoxia and 24-hr hyperoxia cohorts (Table 7). IT saline increased the total cell counts over that of normoxia rats by a factor of ~3, whereas the cell counts increased by a factor of ~30 in BAL from rats 24 hrs after LPS treatment ( $p < 0.05$  saline vs LPS). Differential macrophage, polymorphonuclear neutrophil (PMN), lymphocyte and other cell counts (mostly epithelial and unidentifiable cells) in normoxia and hyperoxia cohorts were not different. IT saline increased PMN percentages over that of normoxia rats. BAL from 24-hr LPS rats had ~ 90% PMNs with the percentage (but not total numbers) of macrophages commensurately less than those of the other three cohorts.

### HMPAO imaging results

Figure 4 shows representative HMPAO images at steady-state obtained from a normoxia rat (A), and from rats 24 hrs after either hyperoxia (B), IT saline (C) or IT LPS (D), where the

lung and background ROIs are outlined. Increased HMPAO lung uptake is evident in the lung region of both the hyperoxia and LPS-treated rats.

Figure 5 shows the time course of the lung uptake (the ratio of lung-to-background signal at steady-state) of HMPAO for the two injury models. For rats exposed to hyperoxia, HMPAO lung uptake increased by 134% and 172% after 24 hrs and 48 hrs of exposure, respectively. For LPS treated rats, HMPAO lung uptake 24 hrs later was 188% higher than that in IT saline rats. Relative to IT saline, the increase in HMPAO lung uptake was significantly lower at 3 days (84%) and 7 days (53%) after LPS treatment. In saline-treated rats, HMPAO lung uptake was not different from that in normoxia rats, indicating that the LPS treatment, and not vehicle (saline) or anesthesia during the LPS instillation procedure, was responsible for increased HMPAO lung uptake.

We investigated the role of GSH in HMPAO lung uptake by imaging rats before and after treatment with the GSH-depleting agent DEM (14). In all groups, DEM treatment resulted in significantly reduced HMPAO uptake (Figure 5, open vs. closed symbols) suggesting the role of GSH in the uptake of HMPAO. For rats exposed to hyperoxia for 24 hrs, the enhanced HMPAO lung uptake was mostly DEM-sensitive. On the other hand, for rats exposed to hyperoxia for 48 hrs, only ~50% of the measured increase in HMPAO lung uptake was DEM-sensitive. Almost all of the increase in HMPAO lung uptake in LPS-treated rats at 24 hrs, 3 days and 7 days was DEM-sensitive.

Table 6 shows the results of the glutathione assays indicating that rat exposure to hyperoxia increased lung tissue GSH content after 24 hrs (17%) of exposure as compared to lungs of normoxia rats. For LPS treated rats, lung tissue GSH content increased at 24 hrs (26%), but not at 7 days after treatment as compared to that in lungs of IT saline alone. Lung GSH content of saline-treated rats was not different from that of normoxia rats, indicating that the LPS treatment, and not vehicle (saline) or anesthesia during the LPS instillation procedure, was responsible for the increase 24 hrs after treatment. The GSH/GSSG ratios in hyperoxia and LPS lungs were not different from those in normoxia lungs. However, the GSH/GSSG ratios for 24-hr LPS lungs was significantly higher than that for IT saline lungs ( $p < 0.05$ ). Figure 6 shows that there is a strong correlation between GSH tissue content measured from lung tissue assay and *in vivo* HMPAO lung uptake determined from imaging.

## DISCUSSION AND CONCLUSIONS

The results of this study demonstrate for the first time a large increase in  $^{99m}\text{Tc}$ -HMPAO lung uptake in the absence of clinically-relevant lung injury 24 hours after hyperoxia-induced ALI or following treatment with a low dose of LPS (Table 8). Moreover, we demonstrated the ability of HMPAO lung uptake to track the progression of hyperoxia-induced ALI and the reversibility of LPS-induced ALI (Figures 1 and 5).

Our choice of injury models and time points was motivated by our long-term goal of developing a means for early clinical detection and monitoring of ALI in individual patients, and by the objectives of this paper which are key first steps towards this goal. Hyperoxia was selected as an injury model because sustained exposure to high fractions of oxygen causes

ARDS in and of itself, and it is an essential therapy for hosts with hypoxemia from any cause (4). For rats exposed to hyperoxia for 24 hrs, the increase in  $^{99m}\text{Tc}$ -HMPAO lung uptake occurred well prior to functional, morphometric or histologic changes known to occur with sustained exposure to hyperoxia based upon heart rate (HR), oxygen saturation, plain films of the chest, BAL protein, cell counts and differentials (Figures 1–3, Tables 1–5, 7). A larger increase in HMPAO lung uptake was measured for rats exposed to hyperoxia for 48 hrs (Figure 5), consistent with the potential of HMPAO lung uptake to track the severity of lung injury, which for this model is related to the exposure period (Figure 1, Tables 1 and 3) (4).

Previously we evaluated the lung uptake of HMPAO in rats exposed to sublethal 60%  $\text{O}_2$  or 85%  $\text{O}_2$  (9,14). Figure 7 shows HMPAO lung uptake as a function of  $\text{O}_2$  concentration. For 60% and 85%  $\text{O}_2$ , HMPAO uptake was greatest at 7 days of exposure and was 50% and 74% higher than the uptake in normoxia rats, respectively, and significantly lower than the uptake in rats exposed to >95%  $\text{O}_2$  for 24 hrs.

Though the pathophysiologic features of clinical sepsis vary depending on underlying conditions and source of infection, we selected a model and time frame to mimic patients presenting with pre-clinical septic lung dysfunction (22). In particular, the low 1 mg/kg LPS dose and IT administration were chosen to result in limited and reversible lung injury and minimal systemic manifestations. This model allowed us to evaluate the utility of HMPAO lung uptake not only for pre-clinical detection of lung injury, but also, as stated above, for tracking the reversibility of the injury (Figure 5). Common findings of LPS injury include lung influx of neutrophils (5,23,24), bronchoalveolar lavage fluid with increased protein and neutrophils (5,23), decreased lung compliance (12), and decreased oxygenation with high doses of LPS (24), some of which we have corroborated here (Table 7). Several authors reported increased lung wet-to-dry weight ratio 24 hrs after endotoxin (23,24), which was not the case in the present study (Table 1). The 44% increase in left lobe wet weight/body weight ratio 24 hours after LPS treatment may be expected to contribute to decreased compliance and tachypnea. Neutrophil influx (Table 7) and inflammatory changes likely account for much of the increase in lung wet weight and increased MPO we observed at 24 hours (Table 5). The fact that we did not see an increase in lung wet-to-dry weight ratio may reflect the low dose or lot of LPS we used, rat strain, or other factors, but is consistent with the absence of increased permeability as quantified by  $K_f$  (Table 3). Rats followed beyond 24 hours exhibited spontaneous recovery by 3 days in functional endpoints perturbed by LPS which included reversal of body weight loss, tachypnea, and lung wet weight (Figure 1, Table 2–Table 3), again consistent with limited data from other investigators on low dose IT LPS in Sprague Dawley rats and a minimal injury model (5,6).

For LPS treated rats,  $^{99m}\text{Tc}$ -HMPAO lung uptake identifies both the injury and recovery phases of this model (Figure 1 and Figure 5). The lung uptake was highest at 24 hrs after LPS treatment (injury phase) and decreased towards normoxia levels during the recovery phase (days 3–7). The increase in HMPAO lung uptake at 24 hrs occurred simultaneously with histological evidence of mild inflammatory changes and increase in lung wet weight consistent with LPS-induced inflammatory cell infiltration, modest and transient tachypnea and decrease in body weight, increase in BAL protein and cell counts, but no clinical

evidence of distress (normal heart rate, oxygen saturation, thoracic X-ray, posture, grooming, activity, color, skin turgor) or increase in microvascular permeability ( $K_f$ ) (Table 1).

We monitored heart rate, oxygen saturation, thoracic X-ray, and respiratory rates (RR) in our rats because they serve as noninvasive indicators of lung function and are routinely measured clinically. Only RR was significantly altered 24 hrs after LPS (+40%) or hyperoxia (-10%) treatment (Table 8). The ~40% increase in RR observed 24 hours after LPS treatment is consistent with the weight loss and decreased food and water intake which reversed in the following 2 days. However, the modest nature of this injury is supported by the relatively limited degree of tachypnea. For comparison with other injuries, rats with radiation pneumonitis after 15 Gy to the thorax increased their respiratory rates to ~200% of baseline (18). Also, in a clinical setting an increase in respiratory rate from 12 to 17 (roughly 40%) may be considered to still fall within the range of normal. Exposure to hyperoxia for 24 hrs on the other hand resulted in a modest, but significant decrease (~10%) in RR. This result is in line with the decrease (29%) in RR reported by Torbati and Reilly (25). They speculated that this hyperoxia-induced decrease in RR could be due to modulation in afferent inputs from lung stretch receptors or peripheral/central chemoreceptors (25). Table 8 shows that clinically relevant measures of lung function/injury were either not altered or differentially altered early in the development of hyperoxia and LPS-induced lung injury. On the other hand, HMPAO lung uptake was substantially higher early in the development of both hyperoxia and LPS-induced lung injury, suggesting the potential utility of HMPAO for early detection of ALI, i.e. prior to evidence of clinical respiratory distress.

For LPS treated rats, we found that almost all of the increase in HMPAO lung uptake at 24 hrs, 3 days, and 7 days was DEM sensitive (Figure 5), i.e. HMPAO lung uptake following DEM treatment was nearly the same as HMPAO uptake in normoxia and saline-treated rats. For rats exposed to hyperoxia, the enhanced uptake of HMPAO after 24 hrs of exposure was also DEM sensitive (Figure 5). However, ~50% of the increase in uptake after 48 hrs of exposure was DEM insensitive. Since DEM is a known glutathione depletor, there is strong evidence from this study and others (14) that a large portion of the increased lung uptake of HMPAO in these two injury models is GSH dependent. The increase in the reduced (GSH) glutathione content of lung homogenate (+18% for 24-hr hyperoxia and +26% for 24-hr LPS compared to normoxia) is lower than the ~130–190% increase in HMPAO lung uptake measured from the *in vivo* images and the ~600% to 900% increase in the DEM-sensitive portion of the HMPAO lung uptake. One explanation for this difference could be the fact that the GSH content reported in this study is the average GSH content of all lung cells and alveolar fluid. Although the results of this study do not provide information regarding the specific types of lung cells contributing to the lung uptake and retention of HMPAO, previous studies have suggested that its retention is predominantly attributable to endothelial cells (26,27), which account for ~50% of lung cells and are in direct contact with blood (4). Other studies have also demonstrated that different cell types have different GSH content, and oxidant stress has different effects on the GSH content of these cells (28,29). For instance, Deneke et al demonstrated that exposure of endothelial cells to hyperoxia (85% O<sub>2</sub> for 48 hours) increased GSH content by 85% (28). On the other hand, neutrophil GSH content is not sensitive to oxidant injury (29), an important consideration in our studies

given the neutrophilic influx in LPS-evoked injury. Thus, depending on the GSH content of the various lung cells and how the GSH content of these cells change in response to exposure to hyperoxia or treatment with LPS, the GSH content in lung homogenate measured in this study may overestimate or underestimate the effect of hyperoxia or LPS on the GSH content of pulmonary capillary endothelial cells.

Other factors that could account for the enhanced HMPAO lung uptake in hyperoxia and LPS-treated rats include reduced thioredoxin (30), mitochondrial and/or cytosolic redox status, and/or capillary endothelial permeability (14,31). The pulmonary endothelial filtration coefficient ( $K_f$ ) did not increase 24 hrs following treatment with hyperoxia or LPS demonstrating that capillary endothelial permeability was unchanged in either model at that time point (Table 3). Thus, the enhanced HMPAO lung uptake observed with these cohorts of rats cannot be attributed directly to increased diffusion of HMPAO across the capillary endothelial barrier. For 48-hr hyperoxia, ~50% of the enhanced HMPAO lung uptake was DEM-insensitive. This component of the enhanced HMPAO uptake could be due to the increased capillary endothelial permeability as measured by pulmonary endothelial filtration coefficient ( $K_f$ ) (Table 3) or altered mitochondrial redox state. Previously, we demonstrated that rat exposure to > 95% O<sub>2</sub> for 48 hrs decreased lung tissue mitochondrial complex I and II activities and altered mitochondrial redox state (32).

Reduced thioredoxin is an effective reductant of disulfides in proteins and peptides such as GSSG and peroxiredoxins, which catalyze the reduction of H<sub>2</sub>O<sub>2</sub> using reduced thioredoxin as the electron donor (30). Thus, reduced thioredoxin could contribute to the DEM-sensitive component of HMPAO lung tissue retention through its effect on GSSG and H<sub>2</sub>O<sub>2</sub>. As such, an increase in the reduced thioredoxin content could also contribute to the difference between the effect of rat exposure to hyperoxia or treatment with LPS on GSH and the DEM-sensitive fraction of the lung retention of HMPAO discussed above. Additional studies would be needed to evaluate the effect of these insults on the lung thioredoxin system (30,33).

This study suggests the potential utility of <sup>99m</sup>Tc-HMPAO, which is in common clinical use, as marker of early ALI under conditions lacking overt clinical evidence of lung injury, and for tracking the progression or reversibility of the injury. Previous studies have reported increased HMPAO lung uptake in subclinical lung injury due to chemotherapy, radiation injury, and inhalation injuries (26,27,34,35), but not within the time frame of 24 hours. Though much work remains before these observations are ready for clinical application, biomarkers to identify patients at risk of ALI are particularly desirable. These markers could permit identification and intervention in patients at increased risk for ALI or ARDS at a phase in these disorders when interventions are most effective, prior to the development of hypoxemia, tachypnea or hypotension. Because HMPAO uptake may track disease severity, it could also be useful for following individual patients over time: those with continuously rising HMPAO uptake might stratify into a group with worsening lung injury whereas those which peak and fall may be on a path to resolution.

Beyond antibiotics, patients at risk for ALI are strong candidates for strategies including limited blood transfusions (to avoid transfusion related lung injury), closer clinical

observation (such as in an intermediate care unit), limitation of inhaled oxygen fractions to levels needed to support vital organ function, but not more, and strict attention to intake and output measurements to limit fluid retention and pulmonary edema while preserving vital perfusion to kidneys, brain and other organs. These interventions are not universally implemented because of risk to benefit ratios in the larger population of persons receiving enhanced fractions of oxygen or who are septic. However with identification of those who have increased probability of disease progression, the risks of the strategies listed above may be acceptable compared to the risks of progressive ARDS and end organ failure.

## Acknowledgments

We thank Ying Gao for her help with LPS administration and tissue assays and Tracy Gasperetti for measuring the breathing rates, food consumption and body weights.

This work was supported by NIH grants 1R01HL116530 (Jacobs, Audi, Clough), 1R15HL129209 (Audi, Clough, Jacobs), and 8UL1TR000055 (CTSI) (Audi, Clough), VA Merit Review Award BX001681 (Jacobs, Audi, Clough), and the Alvin and Marion Birnschein Foundation (Audi, Clough).

## REFERENCES

1. Matthay MA, Zemans RL. The acute respiratory distress syndrome: pathogenesis and treatment. *Annu Rev Pathol.* 2011; 6:147–163. [PubMed: 20936936]
2. Gajic O, Dara SI, Mendez JL, Adesanya AO, Festic E, Caples SM, Rana R, St Sauver JL, Lymp JF, Afessa B, Hubmayr RD. Ventilator-associated lung injury in patients without acute lung injury at the onset of mechanical ventilation. *Crit Care Med.* 2004; 32:1817–1824. [PubMed: 15343007]
3. Reiss LK, Uhlig U, Uhlig S. Models and mechanisms of acute lung injury caused by direct insults. *Eur J Cell Biol.* 2012; 91:590–601. [PubMed: 22284832]
4. Crapo JD, Barry BE, Foscue HA, Shelburne J. Structural and biochemical changes in rat lungs occurring during exposures to lethal and adaptive doses of oxygen. *Am Rev Respir Dis.* 1980; 122:123–143. [PubMed: 7406333]
5. van Helden HP, Kuijpers WC, Steenvoorden D, Go C, Bruijnzeel PL, van Eijk M, Haagsman HP. Intratracheal aerosolization of endotoxin (LPS) in the rat: a comprehensive animal model to study adult (acute) respiratory distress syndrome. *Exp Lung Res.* 1997; 23:297–316. [PubMed: 9202956]
6. Liu F, Li W, Pauluhn J, Trubel H, Wang C. Lipopolysaccharide-induced acute lung injury in rats: comparative assessment of intratracheal instillation and aerosol inhalation. *Toxicology.* 2013; 304:158–166. [PubMed: 23313377]
7. Bannerman DD, Goldblum SE. Mechanisms of bacterial lipopolysaccharide-induced endothelial apoptosis. *Am J Physiol Lung Cell Mol Physiol.* 2003; 284:L899–L914. [PubMed: 12736186]
8. Audi SH, Jacobs ER, Zhao M, Roerig DL, Haworth ST, Clough AV. In vivo detection of hyperoxia-induced pulmonary endothelial cell death using (99m)Tc-duramycin. *Nucl Med Biol.* 2015; 42:46–52. [PubMed: 25218023]
9. Clough AV, Audi SH, Haworth ST, Roerig DL. Differential lung uptake of 99mTc-hexamethylpropyleneamine oxime and 99mTc-duramycin in the chronic hyperoxia rat model. *J Nucl Med.* 2012; 53:1984–1991. [PubMed: 23086010]
10. Sanders AP, Baylin GJ. A common denominator in the etiology of adult respiratory distress syndrome. *Med Hypotheses.* 1980; 6:951–965. [PubMed: 7432254]
11. Merker MP, Audi SH, Lindemer BJ, Krenz GS, Bongard RD. Role of mitochondrial electron transport complex I in coenzyme Q1 reduction by intact pulmonary arterial endothelial cells and the effect of hyperoxia. *Am J Physiol Lung Cell Mol Physiol.* 2007; 293:L809–L819. [PubMed: 17601793]
12. da Cunha MJ, da Cunha AA, Scherer EB, Machado FR, Loureiro SO, Jaenisch RB, Guma F, Lago PD, Wyse AT. Experimental lung injury promotes alterations in energy metabolism and respiratory

- mechanics in the lungs of rats: prevention by exercise. *Mol Cell Biochem.* 2014; 389:229–238. [PubMed: 24378995]
13. Pacht ER, Timerman AP, Lykens MG, Merola AJ. Deficiency of alveolar fluid glutathione in patients with sepsis and the adult respiratory distress syndrome. *Chest.* 1991; 100:1397–1403. [PubMed: 1935300]
  14. Audi SH, Roerig DL, Haworth ST, Clough AV. Role of glutathione in lung retention of 99mTc-hexamethylpropyleneamine oxime in two unique rat Models of hyperoxic lung injury. *J Appl Physiol.* 2012; 113:658–665. [PubMed: 22628374]
  15. Neirinckx RD, Burke JF, Harrison RC, Forster AM, Andersen AR, Lassen NA. The retention mechanism of technetium-99m–HM-PAO: intracellular reaction with glutathione. *J Cereb Blood Flow Metab.* 1988; 8:S4–S12. [PubMed: 3192641]
  16. Herasevich V, Yilmaz M, Khan H, Hubmayr RD, Gajic O. Validation of an electronic surveillance system for acute lung injury. *Intensive Care Med.* 2009; 35:1018–1023. [PubMed: 19280175]
  17. Fu PK, Wu CL, Tsai TH, Hsieh CL. Anti-inflammatory and anticoagulative effects of paeonol on LPS-induced acute lung injury in rats. *Evid Based Complement Alternat Med.* 2012; 2012:837513–837525. [PubMed: 22454687]
  18. Medhora M, Gao F, Glisch C, Narayanan J, Sharma A, Harmann LM, Lawlor MW, Snyder LA, Fish BL, Down JD, Moulder JE, Strande JL, Jacobs ER. Whole-thorax irradiation induces hypoxic respiratory failure, pleural effusions and cardiac remodeling. *J Radiat Res.* 2015; 56:248–260. [PubMed: 25368342]
  19. Szabo S, Ghosh SN, Fish BL, Bodiga S, Tomic R, Kumar G, Morrow NV, Moulder JE, Jacobs ER, Medhora M. Cellular inflammatory infiltrate in pneumonitis induced by a single moderate dose of thoracic x radiation in rats. *Radiat Res.* 2010; 173:545–556. [PubMed: 20334527]
  20. Bongard RD, Yan K, Hoffmann RG, Audi SH, Zhang X, Lindemer BJ, Townsley MI, Merker MP. Depleted energy charge and increased pulmonary endothelial permeability induced by mitochondrial complex I inhibition are mitigated by coenzyme Q1 in the isolated perfused rat lung. *Free Radic Biol Med.* 2013; 65:1455–1463. [PubMed: 23912160]
  21. Densmore JC, Jeziorczak PM, Clough AV, Pritchard KA Jr, Cummens B, Medhora M, Rao A, Jacobs ER. Rattus model utilizing selective pulmonary ischemia induces bronchiolitis obliterans organizing pneumonia. *Shock.* 2013; 39:271–277. [PubMed: 23364425]
  22. Abraham E. Coagulation abnormalities in acute lung injury and sepsis. *Am J Respir Cell Mol Biol.* 2000; 22:401–404. [PubMed: 10745020]
  23. Tong L, Bi J, Zhu X, Wang G, Liu J, Rong L, Wang Q, Xu N, Zhong M, Zhu D, Song Y, Bai C. Keratinocyte growth factor-2 is protective in lipopolysaccharide-induced acute lung injury in rats. *Respir Physiol Neurobiol.* 2014; 201:7–14. [PubMed: 24973472]
  24. Hou S, Ding H, Lv Q, Yin X, Song J, Landen NX, Fan H. Therapeutic effect of intravenous infusion of perfluorocarbon emulsion on LPS-induced acute lung injury in rats. *PLoS One.* 2014; 9:e87826. [PubMed: 24489970]
  25. Torbati D, Reilly KJ. Effect of prolonged normobaric hyperoxia on regional cerebral metabolic rate for glucose in conscious rats. *Brain Res.* 1988; 459:187–191. [PubMed: 3167579]
  26. Kuo SJ, Yang KT, Chen DR. Objective and noninvasive detection of sub-clinical lung injury in breast cancer patients after radiotherapy. *Eur J Surg Oncol.* 2005; 31:954–957. [PubMed: 16102933]
  27. Suga K, Uchisako H, Nishigauchi K, Shimizu K, Kume N, Yamada N, Nakanishi T. Technetium-99m–HMPAO as a marker of chemical and irradiation lung injury: experimental and clinical investigations. *J Nucl Med.* 1994; 35:1520–1527. [PubMed: 8071704]
  28. Deneke SM, Steiger V, Fanburg BL. Effect of hyperoxia on glutathione levels and glutamic acid uptake in endothelial cells. *J Appl Physiol.* 1987; 63:1966–1971. [PubMed: 2891677]
  29. Durak H, Kilinc O, Ertay T, Ucan ES, Kargi A, Kaya GC, Sis B. Tc-99m–HMPAO uptake by bronchoalveolar cells. *Ann Nucl Med.* 2003; 17:107–113. [PubMed: 12790358]
  30. Tipple TE, Welty SE, Nelin LD, Hansen JM, Rogers LK. Alterations of the thioredoxin system by hyperoxia: implications for alveolar development. *Am J Respir Cell Mol Biol.* 2009; 41:612–619. [PubMed: 19244202]

31. Lassen NA, Andersen AR, Friberg L, Paulson OB. The retention of [99mTc]-d,l-HM-PAO in the human brain after intracarotid bolus injection: a kinetic analysis. *J Cereb Blood Flow Metab.* 1988; 8:S13–S22. [PubMed: 3192638]
32. Sepehr R, Audi SH, Staniszewski KS, Haworth ST, Jacobs ER, Ranji M. Novel Fluorometric Tool to Assess Mitochondrial Redox State of Isolated Perfused Rat Lungs after Exposure to Hyperoxia. *IEEE J Transl Eng Health Med.* 2013; 1:1–24.
33. Sano H, Sata T, Nanri H, Ikeda M, Shigematsu A. Thioredoxin is associated with endotoxin tolerance in mice. *Crit Care Med.* 2002; 30:190–194. [PubMed: 11902261]
34. Hung CJ, Liu FY, Shaiu YC, Kao A, Lin CC, Lee CC. Assessing transient pulmonary injury induced by volatile anesthetics by increased lung uptake of technetium-99m hexamethylpropylene amine oxime. *Lung.* 2003; 181:1–7. [PubMed: 12879335]
35. Liu FY, Shian YC, Huang WT, Kao CH. Usefulness of technetium-99m hexamethylpropylene amine oxime lung scan to detect sub-clinical lung injury of patients with breast cancer after chemotherapy. *Anticancer Res.* 2003; 23:3505–3507. [PubMed: 12926098]



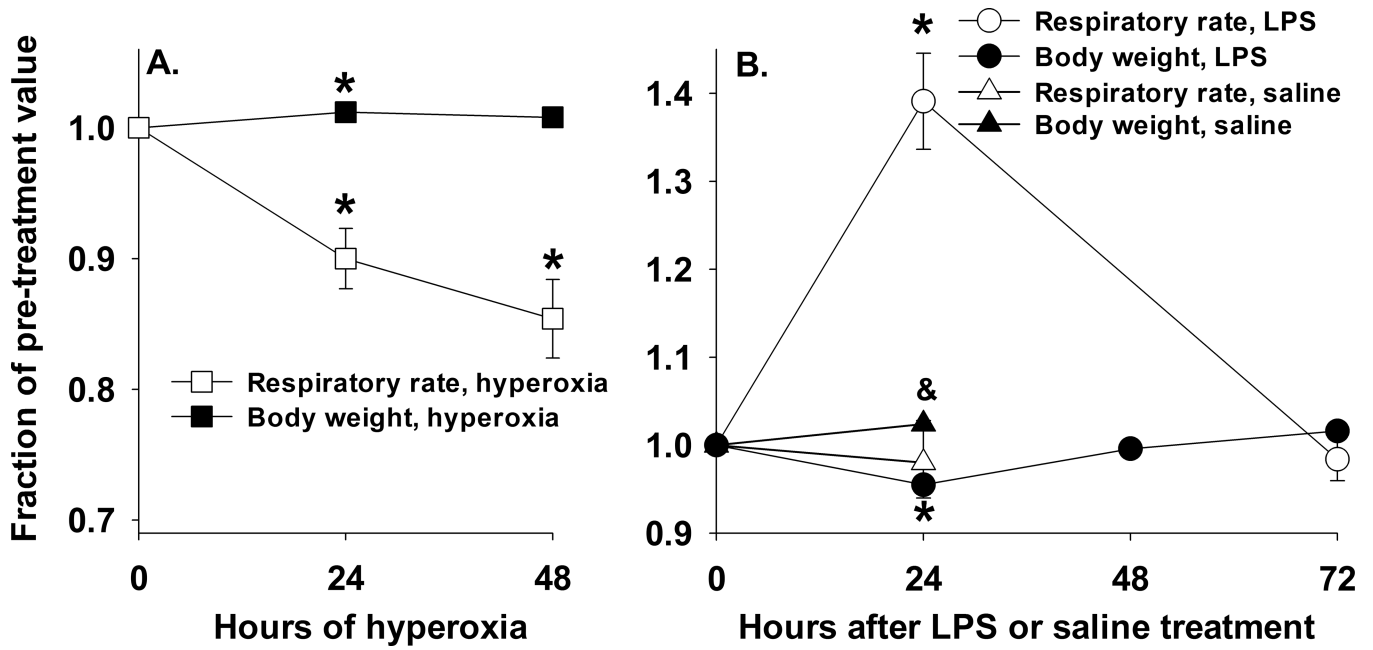


**Figure 1.**

*Panel A.* Rat body weights (BW) and respiratory rates (RR) following exposure to hyperoxia (hyper) for 24 hrs or 48 hrs. Values are mean  $\pm$  SEM,  $n = 6$  for 24-hr hyperoxia and 48-hr hyperoxia. For each rat, BW and RR are expressed as a fraction of those just prior to treatment (0 hrs,  $n = 6$ ). One way repeated measure ANOVA followed by the Tukey's test was used to evaluate differences among the three time points: \* significantly different from day 0 ( $p < 0.05$ ). *Panel B.* Rat BW and RR over a 72 hr period following treatment with LPS or saline (day 0). Values are mean  $\pm$  SEM,  $n = 5$  for LPS treated rats and  $n = 6$  for saline treated rats. For each rat, BW and RR are expressed as a fraction of those just prior to LPS or saline treatment (0 hrs). One way repeated measure ANOVA followed by the Tukey's test was used to evaluate differences among the three or four time points for LPS treated rats: \* significantly different from day 0 ( $p < 0.001$ ). Paired *t-test* was used to evaluate differences in BW or RR before and after saline treatment: & saline (24 hrs) BW significantly different from 0 hrs ( $p < 0.05$ ).

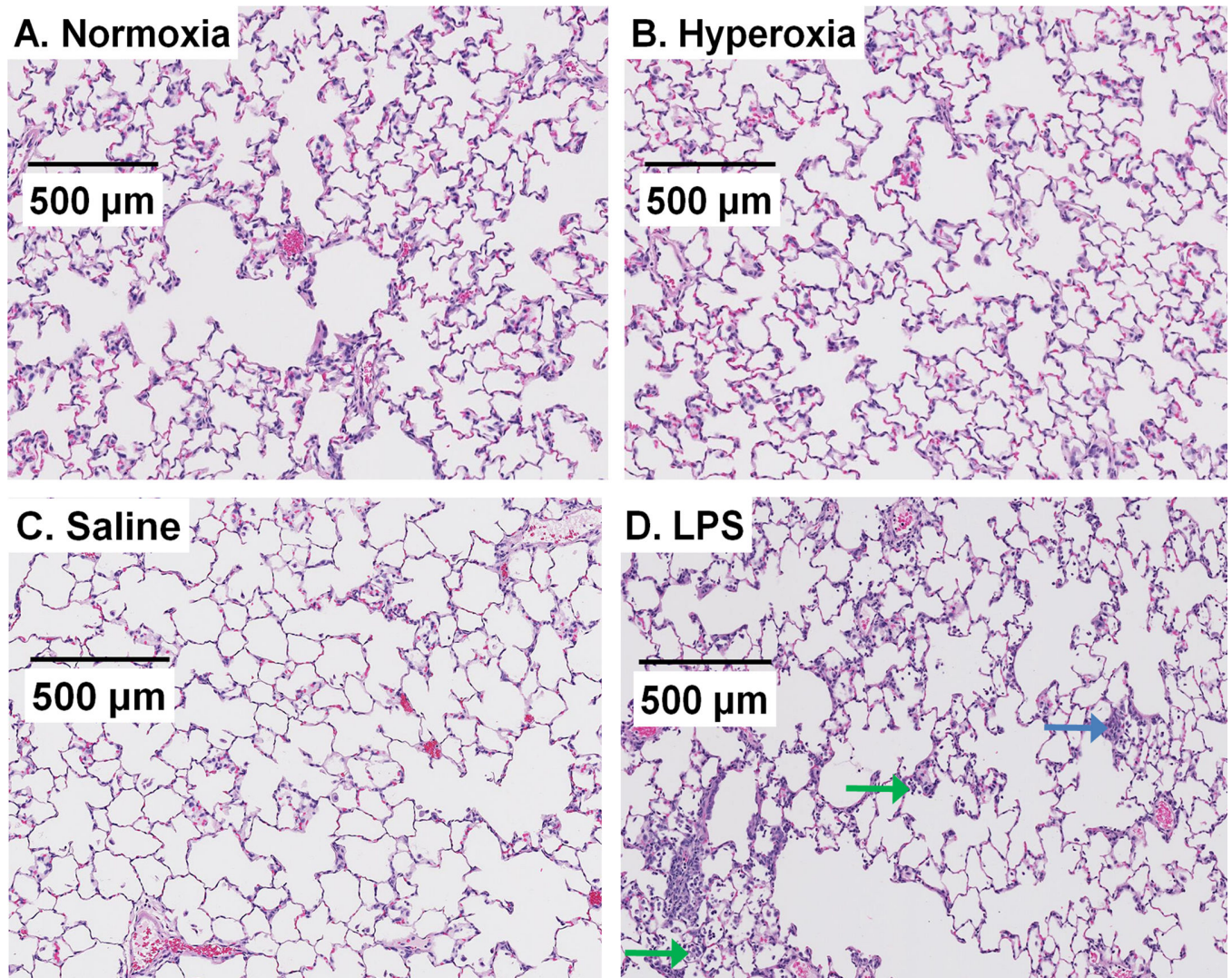


**Figure 2.** Representative images of normoxia (A), 24-hr hyperoxia (B), 24-hr saline (C), and 24-hr LPS (D) H&E stained lung slices. No histological differences were evident in sections from hyperoxia rats. In contrast, many, though not all, sections from rats treated with LPS exhibited scattered inflammatory infiltrates in the interstitium (blue arrow) or alveolar spaces (green arrow).

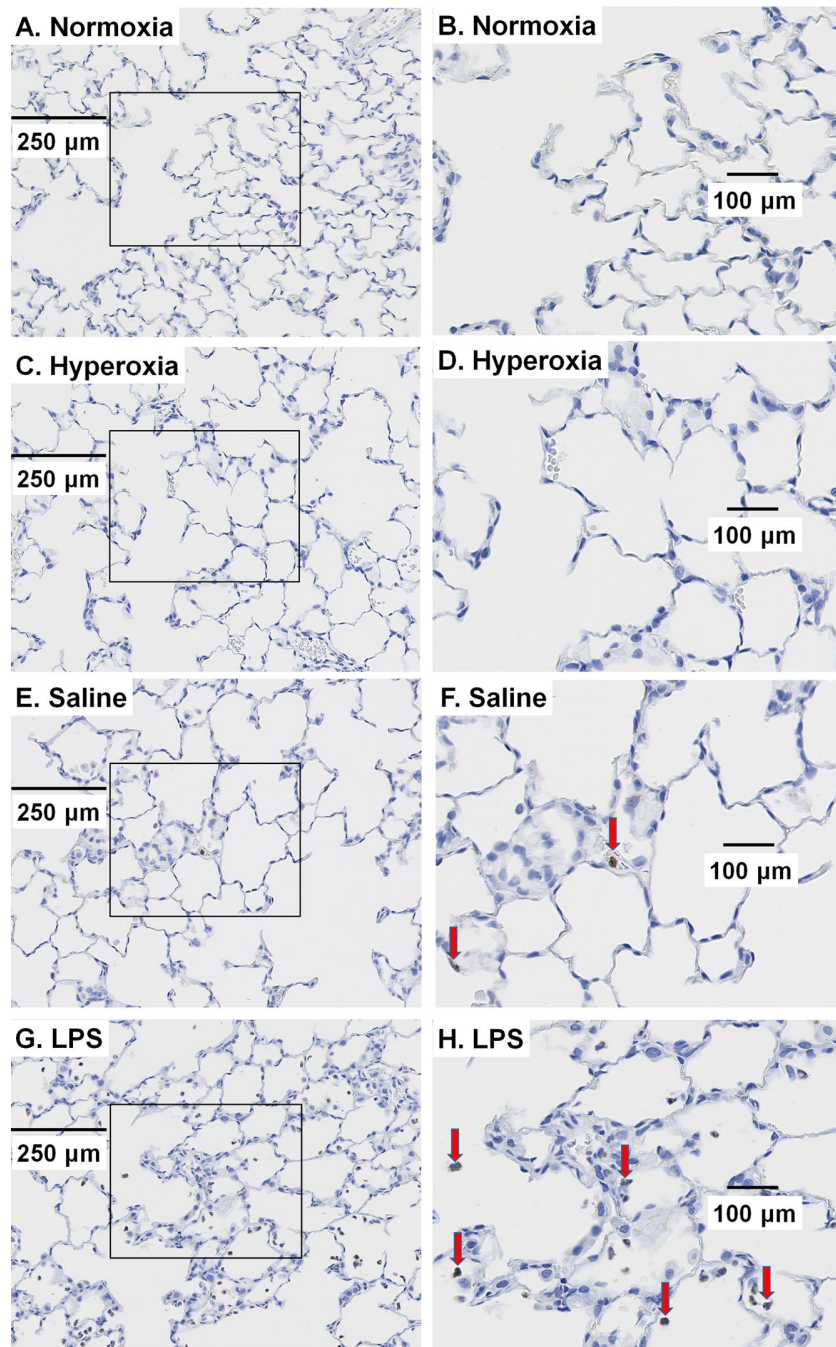


**Figure 3.** Representative sections of normoxia (A), 24-hr hyperoxia (C), 24-hr saline (E), and 24-hr LPS (G) lungs stained with myeloperoxidase (MPO) to identify inflammatory cells. (B, D, F, and H) are enlarged images from the areas demarcated by squares in (A, C, E, and F, respectively) to more clearly demonstrate the brown MPO staining in the cytoplasm of inflammatory cells. The red arrows identify MPO positive cells.

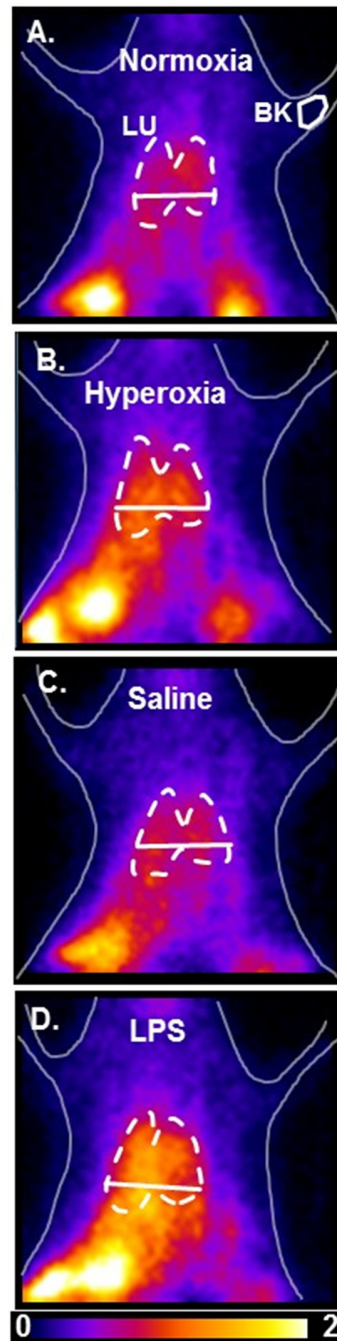


**Figure 4.** Planar images of  $^{99m}\text{Tc}$ -HMPAO distribution in a normoxia (A), 24-hr hyperoxia (B), 24-hr saline (C), and 24-hr LPS (D) rat 20 min after HMPAO injection (pre-DEM). Lung (LU) ROI is determined from the MAA image with the solid horizontal lower boundary used to avoid liver contribution, and background (BK) ROIs from upper forelimb.

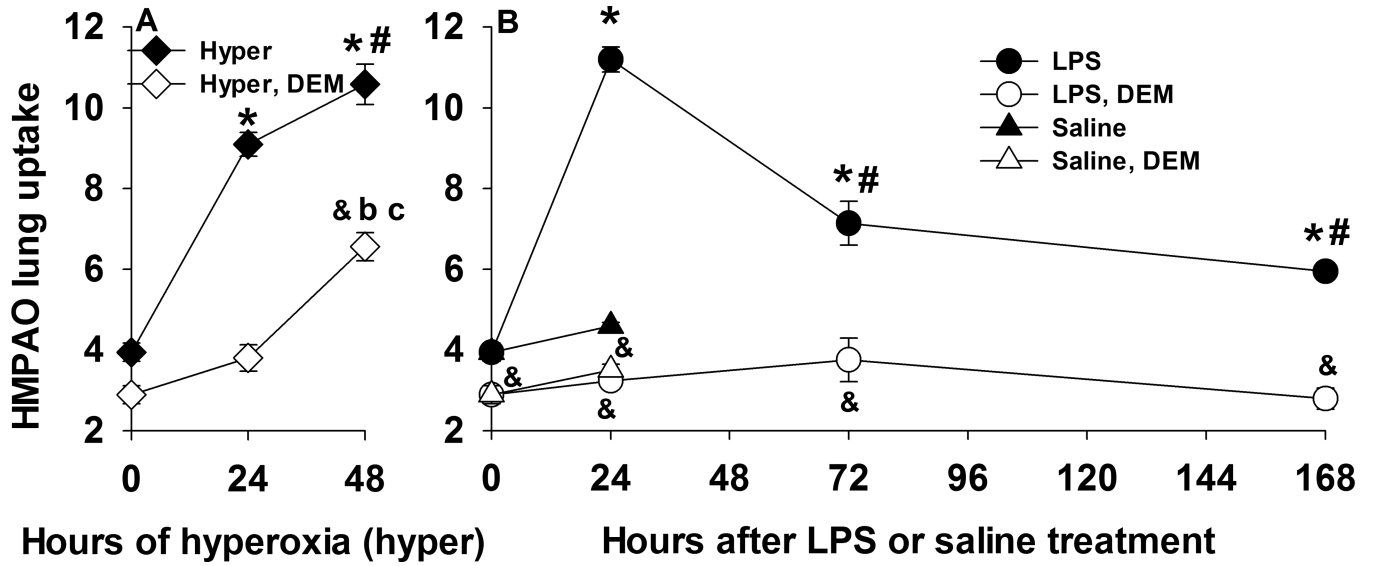


**Figure 5.**

*Panel A.*  $^{99m}\text{Tc}$ -HMPAO lung uptake in normoxia ( $n = 8$ ), 24-hr hyperoxia ( $n = 6$ ), and 48-hr hyperoxia ( $n = 5$ ) rats before (closed symbols) and after (open symbols) treatment with DEM. \*different from normoxia pre DEM; # different from 24-hr hyperoxia pre DEM; & different from pre DEM for a given group of rats; <sup>b</sup> different from normoxia post DEM; <sup>c</sup> different from 24-hr hyperoxia post DEM. *Panel B.*  $^{99m}\text{Tc}$ -HMPAO lung uptake in normoxia ( $n = 8$ ), 24-hr saline ( $n = 5$ ) and LPS ( $n = 6$ ), 72-hr LPS ( $n = 4$ ), and 168-hr LPS ( $n = 4$ ) rats before (closed symbols) and after (open symbols) treatment with DEM. Values are mean  $\pm$  SEM. \*different from normoxia pre DEM; # different from 24-hr LPS pre DEM; & different from pre DEM for a given group of rats. One-way ANOVA followed by Tukey's range test ( $p < 0.05$ ) was used to evaluate differences among the three groups for panel A. and among means of the five groups for panel B. Paired  $t$ -test ( $p < 0.05$ ) was used to evaluate difference pre and post DEM for a given group.

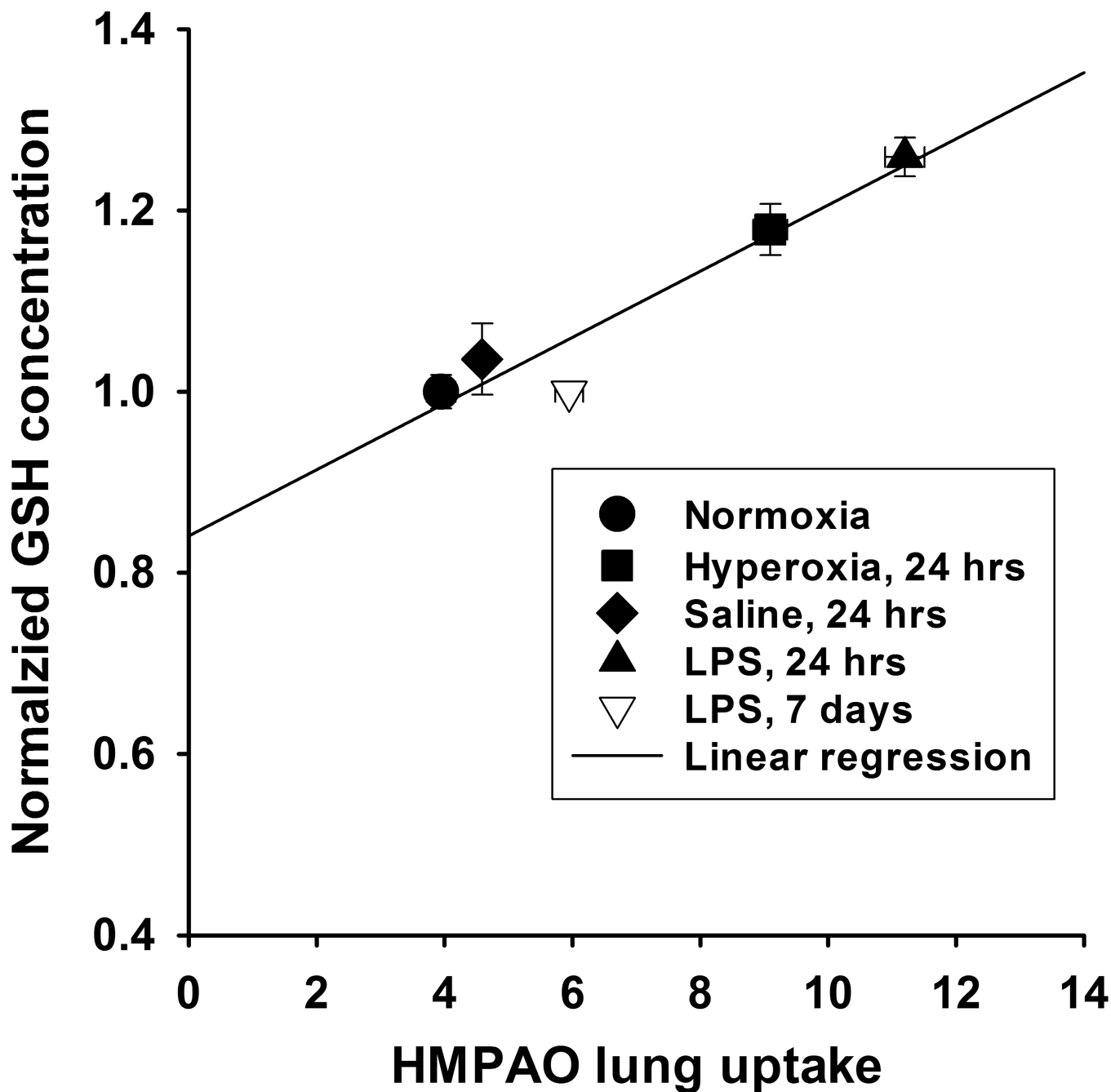


**Figure 6.** Correlation between  $^{99m}\text{Tc}$ -HMPAO lung uptake (Figure 5) and lung tissue GSH content (as fraction of normoxia, Table 6). Values are mean  $\pm$  SEM. Solid line is linear model fit ( $r^2 = 0.92$ , Pearson Product Moment Correlation test,  $p = 0.01$ ).

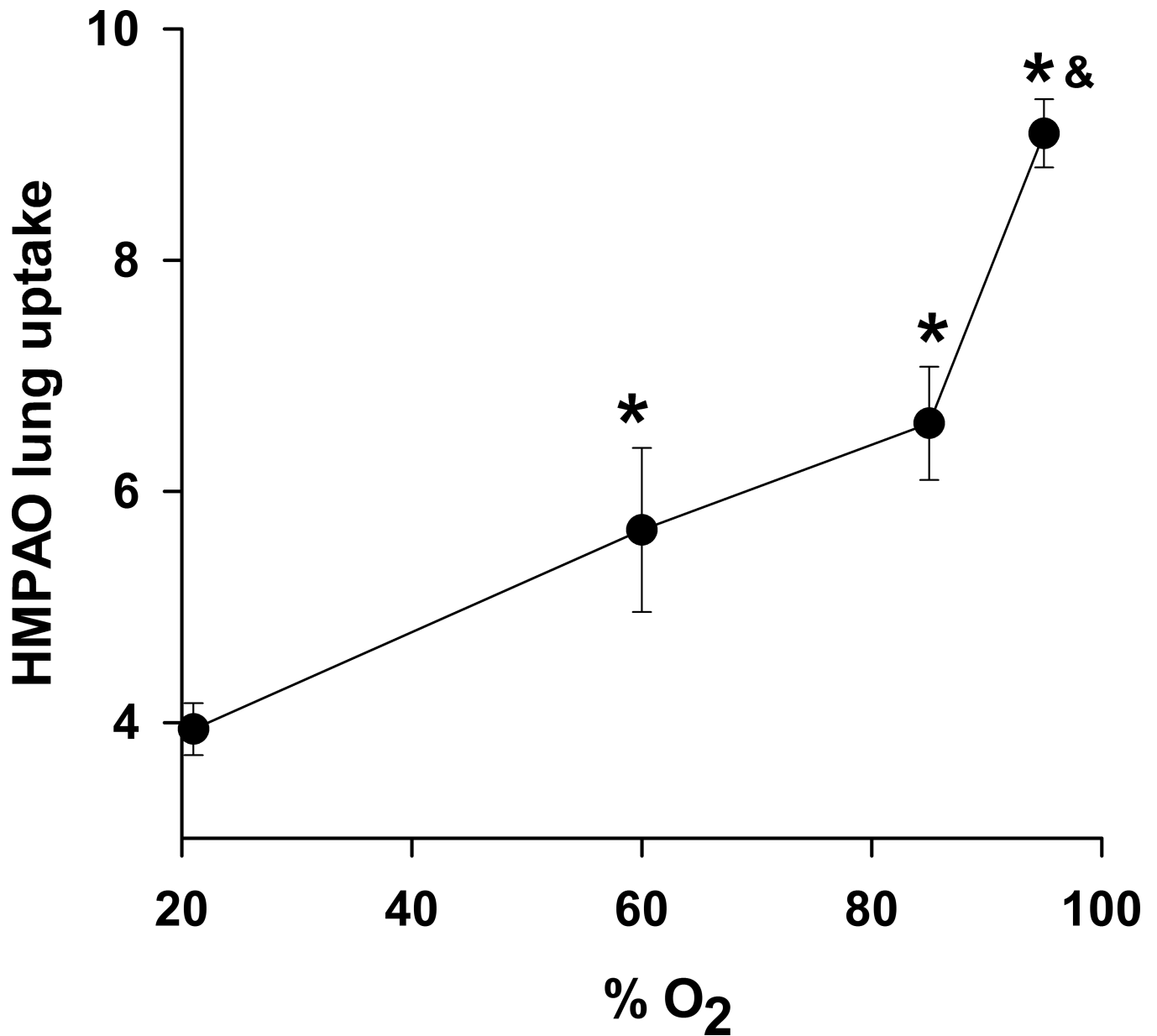


**Figure 7.** <sup>99m</sup>Tc-HMPAO lung uptake in normoxia rats (n = 8), and in rats exposed to 60% O<sub>2</sub> for 7 days (n = 4) (14), 85% O<sub>2</sub> for 7 days (n = 5) (9), or >95% O<sub>2</sub> for 24 hrs (n = 6). \*different from normoxia; & different from 7-day 60% O<sub>2</sub> and 7-day 85% O<sub>2</sub> (one-way ANOVA followed by Tukey's range test, *p* < 0.05).

**Table 1**

Body weight pre and post treatment

Treatment	Pre-body wt (g)	Post-body wt (g)
24-hr hyperoxic (n = 32)	341 ± 5	347 ± 4 *
48-hr hyperoxic (n = 23)	340 ± 5	333 ± 5 *
24-hr saline (n = 29)	331 ± 9	322 ± 9
24-hr LPS (n = 41)	330 ± 7	309 ± 6 *
3-day LPS (n = 8)	350 ± 3	348 ± 5
7-day LPS (n = 7)	352 ± 4	376 ± 7 *

Values are mean ± SE. n is the number of rats.

\* significantly different from the corresponding pre-body weight (paired *t*-test or Wilcoxon Signed Rank Test, *p* < 0.05).

Author Manuscript

Author Manuscript

Author Manuscript

Author Manuscript



**Table 2**

Heart rates (HR) and oxygen saturation (pulse Ox)

Treatment	HR (bpm)	Pulse Ox (% saturation)
Normoxia (n = 9)	394 ± 9	95.5 ± 0.4
24-hr hyperoxia (n = 4)	423 ± 4	94.2 ± 0.7
48-hr hyperoxia (n = 4)	394 ± 5	93.4 ± 0.3*
24-hr saline (n = 3)	384 ± 37	92.6 ± 0.8
24-hr LPS (n = 6)	336 ± 16*	94.5 ± 1.0

Values are Mean ± SE. n is the number of rats.

\* Different from normoxia (ANOVA,  $p < 0.05$ )

**TABLE 3**Lung weights and vascular endothelial filtration coefficient ( $K_f$ )

	Left lobe wet weight/body weight ( $\mu\text{g/g}$ )	Left lobe wet/dry ratio	$K_f$ (ml/min/cmH <sub>2</sub> O/g dry lung wt)
<b>Normoxia</b>	1.22 $\pm$ 0.03 n = 8	5.22 $\pm$ 0.09 n = 8	0.0275 $\pm$ 0.0024 n = 6
<b>24-hr hyperoxia</b>	1.21 $\pm$ 0.04 n = 6	4.77 $\pm$ 0.08 n = 6	0.0241 $\pm$ 0.0068 n = 6
<b>48-hr hyperoxia</b>	1.60 $\pm$ 0.08* n = 16	5.70 $\pm$ 0.15 n = 16	0.0860 $\pm$ 0.0129* n = 6
<b>24-hr saline</b>	1.24 $\pm$ 0.04 n = 5	4.99 $\pm$ 0.15 n = 5	0.0324 $\pm$ 0.0056 n = 5
<b>24-hr LPS</b>	1.79 $\pm$ 0.10& n = 6	5.14 $\pm$ 0.05 n = 6	0.0192 $\pm$ 0.0021 n = 5
<b>3-day LPS</b>	1.45 $\pm$ 0.10 n = 4	4.86 $\pm$ 0.05 n = 4	NA
<b>7-day LPS</b>	1.44 $\pm$ 0.06 n = 3	5.36 $\pm$ 0.11 n = 3	NA

Values are mean  $\pm$  SEM. n is the number of rats. One-way ANOVA on Ranks followed by Tukey's range test ( $p < 0.05$ ) was used to evaluate differences among means of the groups:

\* significantly different from normoxia;

& different from saline.

H&E inflammation analysis

TABLE 4

Group	Median	25%	75%	<i>p</i> < 0.05 vs. Normoxia	<i>p</i> < 0.05 vs. Saline
Normoxia (n = 5)	0	0	0	-	no
24-hr hyperoxia (n = 5)	0	0	0	no	no
24-hr saline (n = 4)	0.3	0.2	0.6	no	-
24-hr LPS (n = 5)	0.9	0.5	1.4	yes	no

Inflammatory changes were scored on a 0–3 scale (21): 0 = no inflammation; 1 = mild perivascular or peribronchiolar inflammatory infiltrates; 2 = moderate mixed inflammatory infiltrates throughout the lung; 3 = severe infiltration of mixed inflammatory cells. n is the number of rats. Images were scored independently by two investigators blinded to the treatment groups and compared by ANOVA on ranks.

**TABLE 5**

## Myeloperoxidase (MPO) analysis

Group (n)	Median	25%	75%	<i>p</i> < 0.05 vs. Normoxia	<i>p</i> < 0.05 vs. Saline
Normoxia (n = 5)	0	0	0	-	no
24-hr hyperoxia (n = 5)	0	0	0	no	no
24-hr saline (n = 4)	1.9	0.6	4.4	no	-
24-hr LPS (n = 5)	9.6	3.1	20.0	yes	no

Numbers of MPO positive cells per field were counted by reviewers blinded to the treatment group and compared by ANOVA on ranks. n is the number of rats. Images from LPS-treated rats exhibited more MPO cells than normoxia rats, consistent with neutrophil infiltration.

**TABLE 6**

Reduced (GSH) and oxidized (GSSG) glutathione content of lung homogenate

	<b>GSH (fraction of normoxia)</b>	<b>GSH/GSSG</b>
<b>Normoxia (n = 7)</b>	1.00	20.0 ± 3.5
<b>24-hr hyperoxia (n = 6)</b>	1.17 ± 0.03 *	23.6 ± 1.9
<b>24-hr saline (n = 4)</b>	1.04 ± 0.02	12.7 ± 1.1
<b>24-hr LPS (n = 6)</b>	1.26 ± 0.02 * $\&$	36.9 ± 7.4 $\&$
<b>7-day LPS (n = 3)</b>	1.00 ± 0.01	10.8 ± 1.1

Values are mean ± SEM. n is the number of rats. One-way ANOVA on Ranks followed by Tukey's range test ( $p < 0.05$ ) was used to evaluate differences among means of the five groups:

\* significantly different from normoxia;

$\&$  different from saline. GSH concentration for normoxia lungs was  $7.81 \pm 0.63$  (SEM,  $n = 7$ )  $\mu\text{mol/g}$  dry wt.

**Table 7**

BAL protein, cell counts, and cell types

	Normoxia	24-hr hyperoxia	24-hrs saline	24-hr LPS
<b>Protein</b> (Mean $\pm$ SEM, mg/ml)	0.73 $\pm$ 0.04 n = 5	0.68 $\pm$ 0.10 n = 5	0.78 $\pm$ 0.02 n = 4	1.24 $\pm$ 0.09 <sup>*&amp;</sup> n = 7
<b>Cell count (x 10<sup>4</sup>) in collected BAL fluid</b> (Mean $\pm$ SEM)	99 $\pm$ 25 n = 5	90 $\pm$ 20 n = 5	334 $\pm$ 33 <sup>*</sup> n = 4	3301 $\pm$ 1178 <sup>*&amp;</sup> n = 7
<b>Differential</b> (Mean $\pm$ SEM %)				
<b>Macrophages</b>	80.0 $\pm$ 3.6 n = 5	70.2 $\pm$ 6.0 n = 5	48.4 $\pm$ 7.1 <sup>*</sup> n = 4	7.7 $\pm$ 2.2 <sup>*&amp;</sup> n = 4
<b>Neutrophils</b>	5.3 $\pm$ 2.1 n = 5	8.3 $\pm$ 1.3 n = 5	37.6 $\pm$ 7.9 <sup>*</sup> n = 4	89.7 $\pm$ 1.4 <sup>*&amp;</sup> n = 4
<b>Lymphocytes</b>	11.3 $\pm$ 5.3 n = 5	15.1 $\pm$ 2.3 n = 5	8.1 $\pm$ 2.3 n = 4	1.5 $\pm$ 0.3 <sup>*</sup> n = 4
<b>Others</b>	3.3 $\pm$ 1.1 n = 5	6.5 $\pm$ 3.2 n = 5	5.9 $\pm$ 1.5 n = 4	1.0 $\pm$ 0.7 <sup>&amp;</sup> n = 4

n is the number of rats. One-way ANOVA or one-way ANOVA on Ranks followed by Tukey's range test ( $p < 0.05$ ) was used to evaluate differences among normoxia, saline, and LPS groups.

<sup>\*</sup> different from normoxia;

<sup>&</sup> different from saline.

Summary of changes in clinically-relevant indices of lung function and HMPAO lung uptake in rats 24 hrs after treatment with hyperoxia, saline, or LPS as compared to normoxia rats

**Table 8**

	BR	HR	Pulse Ox	Thoracic X-ray	BW	BAL protein	BAL cell count	HMPAO Lung uptake
24-hyperoxia	-10%	NS	NS	NS	+1.9%	NS	NS	+135%
24-hr saline	NS	NS	NS	NS	NS	NS	+300%	NS
24-hr LPS	+40%	NS	NS	NS	-6.2%	+70%	+3,000%	+188%

% change from normoxia. NS, not significant